

The $H\beta$ Chromospheric Magnetic Field in a Quiescent Filament *

Xing-Ming Bao and Hong-Qi Zhang

National Astronomical Observatories, Chinese Academy of Sciences, Beijing 100012;
baoxm@sun10.bao.ac.cn

Received 2002 October 23; accepted 2002 December 12

Abstract We observed the line-of-sight magnetic field in the chromosphere and photosphere of a large quiescent filament on the solar disk on September 6, 2001 using the Solar Magnetic Field Telescope in Huairou Solar Observing Station. The chromospheric and photospheric magnetograms together with $H\beta$ filtergrams of the filament were examined. The filament was located on the neutral line of the large scale longitudinal magnetic field in the photosphere and the chromosphere. The lateral feet of the filament were found to be related to magnetic structures with opposite polarities. Two small lateral feet are linked to weak parasitic polarity. There is a negative magnetic structure in the photosphere under a break of the filament. At the location corresponding to the filament in the chromospheric magnetograms, the magnetic strength is found to be about 40–70 Gauss (measuring error about 39 Gauss). The magnetic signal indicates the amplitude and orientation of the internal magnetic field in the filament. We discuss several possible causes which may produce such a measured signal. A twisted magnetic configuration inside the filament is suggested.

Key words: Sun: chromosphere — Sun: filaments — Sun: magnetic fields

1 INTRODUCTION

Solar filaments are cool condensations embedded in the hot corona. The formation, maintenance and eruption of filaments are controlled by the evolution of the configuration of the magnetic field. The large-scale orientation of a quiescent filament is usually determined by the background magnetic field in the photosphere (Parker 2001). The magnetic field of filaments in the photosphere was first observed by Babcock & Babcock (1955), and later by Harword (1959). They reported that the filaments are always found above the inversion line of the vertical photospheric magnetic field. The fine structure of the shape and the lateral feet of a filament are affected seriously by the small-scale, weak magnetic polarity near and under the filament in the photosphere. Recently the relationship between the lateral feet of filaments and

* Supported by the National Natural Science Foundation of China.

the photospheric magnetic fields was studied by Martin & Echols (1994) who found that the lateral feet are related to the patches of parasitic polarity. Aulanier et al. (1999) pointed out that the shape and evolution of the lateral feet of filaments are linked to the parasitic polarity.

In the 1960s, the longitudinal component of the magnetic field in quiescent prominences was measured directly with magnetographs using the Zeeman effect on some chromospheric spectral lines (Rust 1966; Harvey 1969; Tandberg-hanssen 1970). They found that the mean strength of magnetic field is less than 10 Gauss and the field is parallel to the solar surface. Zeeman-effect measurements can only give the longitudinal component of the magnetic field. The Hanle-effect measurements, on the other hand, can give all three components from polarization measurements in two spectral lines. Measurement of the magnetic field of prominences using the Hanle effect indicated that the field is nearly horizontal (Athay et al. 1983), and its strength is nearly homogeneous, though it slightly increases with height (Leroy 1989). Three basic prominence models have been summarized by Gilbert et al. (2000) that explain how cool, dense prominences can be supported in the surrounding hot coronal plasma: the normal polarity dip model (Kippenhahn & Schlüter 1957), the normal polarity flux rope model (Hirayama 1985; Leroy 1989), and the inverse polarity flux rope model (Kuperus & Raadu 1974). In all three models, the magnetic tension force provides the support for the cool, dense material.

Both observational and theoretical models indicate that the magnetic field in the prominences is mainly horizontal. However, this result is almost exclusively obtained from measurements of prominences appearing near in the solar limb. Up to now, there are few dedicated observations of line-of-sight magnetic field of filaments in the chromosphere. In this paper, $H\alpha$ and $H\beta$ filtergrams of a quiescent filament, and magnetograms in $H\beta$ and $\text{FeI } 5324.19 \text{ \AA}$ are examined. The objective of this study is to compare the magnetic structure of the filament in the photosphere and chromosphere and discuss the observed magnetic signal in the $H\beta$ magnetograms.

2 OBSERVATION AND DATA REDUCTION

On September 6, 2001, a large quiescent filament was observed by the Solar Magnetic Field Telescope (SMFT) at Huairou Solar Observing Station (HSOS) of National Astronomical Observatories of China. The SMFT has a Cassegrain optical system with a vacuum tube, a birefringent filter, a CCD camera and a image processor controlled by personal computer. The diameter of the objective is 35cm and its focal length is 280cm (Ai & Hu 1986). The tunable birefringent filter is used for quasi-simultaneous observation of the chromospheric magnetic field at -0.24 \AA from the $H\beta \lambda 4861.34 \text{ \AA}$ line and of the photospheric magnetic field at -0.075 \AA from the center of $\text{FeI } 5324.19 \text{ \AA}$. During the taking of the magnetograms, the right and left circular polarizations pass through the filter, charging the KD^*P crystal with a periodic voltage. The modulation frequency of the KD^*P is 50 Hz.

The strength of the longitudinal magnetic field is derived from

$$B_{\parallel} = C \frac{I_1 - I_2}{I_1 + I_2}, \quad (1)$$

where C is the calibration coefficient of the longitudinal magnetic field, I_1 and I_2 are the intensities of the right and left circular polarizations.

An empirical calibration method of $\text{FeI } 5324.19 \text{ \AA}$ line and $H\beta \lambda 4861.34 \text{ \AA}$ line was introduced by Wang et al. (1996). The field of view is $4.07' \times 2.77'$. The recording system uses a CCD with 512×512 pixels and one pixel corresponds to about 0.5 arcsecond. Before measuring

the magnetic field, a filtergram is usually saved as a 512×512 array in a 8-bit digital file by a 151 series image processor (called image box). In order to increase the sensitivity of measurement, each magnetogram was constructed as follows: 256 filtergrams from right and left polarizations modulated by KD*P are grabbed alternately, and are summed to give I_1 and I_2 . The integration time is about 40 seconds. This method minimizes the image motion due to the Earth's atmosphere between the right and left polarization measurements, each pair being separated only by 20 ms in time. The strength of magnetic field is in fact proportional to the sum of the differences within each of the pairs of frame (such as the 10th frames of I_1 and I_2) even though, for example, there may be large image motion between the first and last frames. The magnetograms are saved as a 16-bit image intensity file (labelled DAT) calculated according Equation (1).

Table 1 lists the observed data of the filament, including the H β filtergrams, and the H β and photospheric magnetograms. Additionally, a 14cm H α telescope (Deng et al. 1997) was used to obtain the H α filtergrams of the full disk and the local region. Some of the data (labelled DAD) only stored the images of I_1 and I_2 . One aim here is to verify if the two images of I_1 and I_2 are lined up through a correlation calculation by Fast Fourier Transform, because the two images of I_1 and I_2 have the same pixel size (512×512) and quite similar features (Fig. 1a and 1b, see Plate II), though there is a difference between their intensities, and the difference is expressed in the Stokes parameter V , from which the line-of sight magnetic field is inferred (Fig. 1c, see Plate II). The principle of the correlation calculation is that all the features in two images with a similar geometric configuration will shift by the same distance and same direction if there is any motion between the two images. The shift distances x and y (in two orthogonal direction) are obtained when the correlation coefficient is at maximum. If both x and y are zero, then the two images are considered to be lined up within one pixel. We have verified that the two images in Fig. 1a and 1b are lined up through the correlation reduction. Figure 1d shows the average of Fig. 1a and 1b (half of their sum) and can be taken as the filtergram of the filament. Thus we can superpose the profile of the filament of the H β filtergrams to the chromospheric magnetograms because the two images are in fact derived from the same two images. The profile of the filament can also be superposed on other chromospheric magnetograms through the correlation reduction if we assume the configuration of the network magnetic field does not change greatly in 1 or 2 hours. Zhang & Zhang (2000) compared the longitudinal magnetic field in the chromosphere and photosphere in quiescent regions observed by SMFT. They found similarity between the chromospheric and photospheric fields. This allows us to make the correlation reduction between the chromospheric and photospheric fields and superpose the profile of the filament in the H β filtergram on the photospheric magnetograms. We can also make the superposition through FFT.

The filament appeared from the eastern edge of the solar disk on September 2, 2001. A height 20 000 km can be inferred from the configuration of the prominence near the solar limb. The filament extended about 6 arcmin along the east-west direction on September 6 (Fig. 2a). It was located between N15°–27° in latitude, and E35°–65° in longitude. The H α filtergram (Fig. 2b) shows a close-up view of the filament. The H β filtergram (Fig. 3a, see Plate III) shows the main body of the filament with several lateral feet (include the two large ones F1 and F2). The main body of the filament has two distinguishable sections: a smooth and homogeneous east section is and an irregular west section, the two separated by a break point labelled D. The filament disappeared on Sep. 9 as a new magnetic flux emerged to its east.

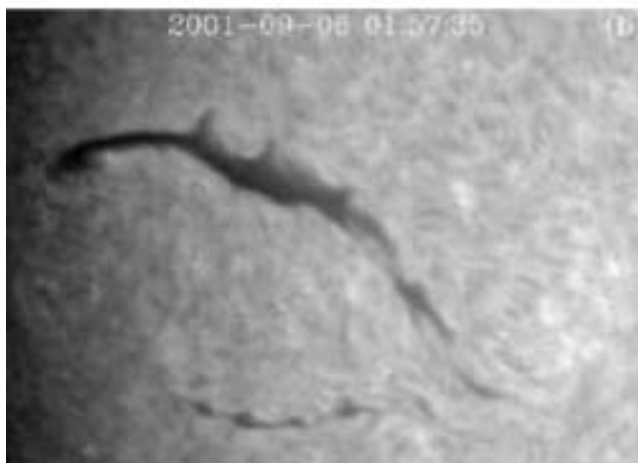
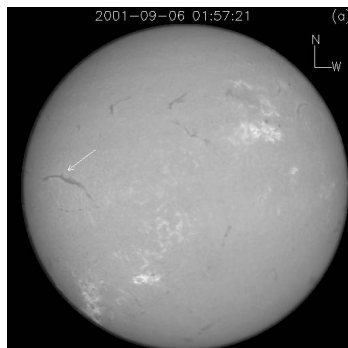


Fig. 2 Filtergrams of the filament on Sep. 6, 2001. (a) Full disk image of $H\alpha$ filtergram at 01:57:21 UT. The arrow points out the filament. (b) Local image of $H\alpha$ filtergram at 01:57:35 UT, the field of view is $8.0' \times 5.75'$.

The $H\beta$ filtergram and photospheric magnetogram of the filament are shown in Fig. 3 (see Plate III). At nearly same time, the large lateral foot F1 divided the filament into two sections: the eastern section is smooth and concentrated, the western section is irregular and diffused. The two large lateral feet F1 and F2 are to the north of the filament, and the two smaller lateral feet F3 and F4 are to the south.

Table 1 Observations of the Filament on 2001 September 9

Time (UT)	Obs. content	Cadence
00:48–00:53	L4. dat	~ 1 min
01:55–02:00	L4. dat	~ 1 min
02:55–03:00	L4. dat	~ 1 min
01:03–01:08	L5. dat	~ 1 min
01:14–01:17	L5. dat	~ 1 min
02:04–02:14	L5. dat	~ 1 min
03:04–03:13	L5. dat	~ 1 min
00:54–00:55	L4. dad	~ 1 min
02:01–02:02	L4. dad	~ 1 min
03:01–03:02	L4. dad	~ 1 min

L4: longitudinal component of magnetic field at H β 4861 Å

L5: longitudinal component of magnetic field at FeI 5324 Å

dat: magnetogram or Dopplergram

dad: file which stores images of the intensity of right and left circular polarization.

Figure 3b is one of the photospheric magnetograms in the FeI 5324.19 Å line, taken at 02:04:29 UT on Sep. 6, 2001. The outline of the filament is superposed on the magnetogram (white solid line). Two magnetic regions with opposite polarities were on the two sides of the filament. The magnetic field near points A and B is the stronger network magnetic field with opposite polarity. There is no any magnetic structure under the filament except at point D, the point where the filament is broken. The parasitic polarity can be found near the end of the two lateral feet F1 and F2. They form a bipolar structure with opposite polarity on the two sides of the lateral feet, and these two opposite polarities correspond to two dark fibers in the H β filtergram (Fig. 3a). Very weak parasitic polarity is found near the two smaller feet F3 and F4. This implies that the lateral feet are closely associated with parasitic polarity.

H β chromospheric magnetograms of the filament are shown in Fig. 4 (see Plate IV). The outline of the filament in the H β filtergram is superposed here (white dashed line). The yellow (blue) contours mark positive (negative) magnetic fields of 40 and 80 Gauss. The network magnetic field near points A and B are similar to that in the photospheric magnetogram (Fig. 3b). Furthermore, the features in the chromospheric magnetograms are also similar to the ones in the H β filtergrams. Zhang et al. (1991) found that the dark fibers in H β filtergram correspond to H β and photospheric magnetic structures. From Fig. 1 and Fig. 4, we also can find some magnetic signatures co-spatial with the H β dark fibers. Because the noise level is greater in the H β magnetograms than in the photospheric magnetograms, the parasitic polarities near the lateral foot look almost vanishingly small except the two positive polarity patches near F1 and F3. In Fig. 4a magnetic signal appears in the location of the filament, especially in its east section. The strength of the field is 40–70 Gauss with both positive and negative polarities. The magnetic polarity at the location of the filament became uniformly negative at 01:58:31 UT (Fig. 4b). The magnetic polarity at the location of the filament in Fig. 4c is opposite to that in Fig. 4a at 00:51:28 UT. The magnetic field is weaker in the west section of the filament than in the east section. The magnetic polarity in the west section also changed with time.

The one-dimensional distribution of the magnetic field intensity along the meridian direction is shown in Fig. 5. The position is marked with a white line in the H β magnetogram (Fig. 4a).

From this plot, we can compare the magnetic field in the filament and the background noise. The strength of magnetic field in the filament reached as high as 70 Gauss or more. The 3σ noise level is about 39 Gauss. It is obvious that the magnetic signal of the filament exceeds the noise level of the magnetogram.

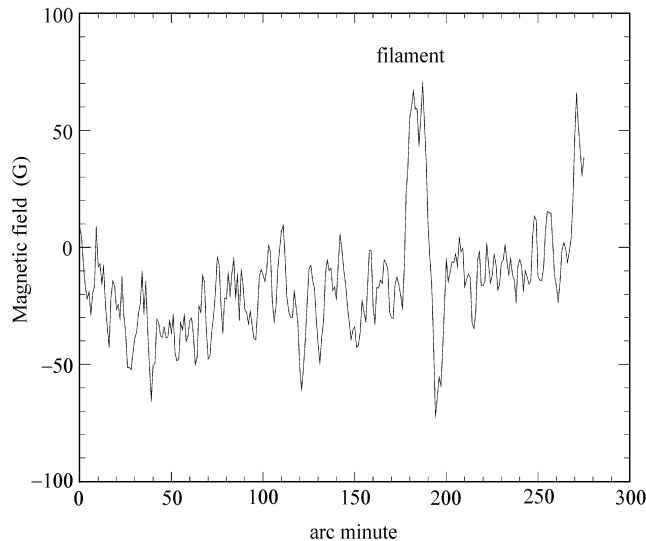


Fig. 5 One dimensional distribution of the magnetic field intensity (Gauss) along the yellow line indicated in magnetogram (Fig. 4a).

3 DISCUSSION AND CONCLUSIONS

We have compared the $H\alpha$ and $H\beta$ filtergrams with the photospheric and chromospheric magnetograms in the vicinity of a large filament. Generally the orientation of the filament is dominated by the configuration of the background magnetic field in the photosphere. Two large lateral feet and several small feet are connected to the main body of the filament. This gives us a very good example for studying the relationship between lateral feet and the magnetic field. The bipolar structure with opposite polarity is found at the end of the two large lateral feet (Fig. 3b). The parasitic polarity appears near the end of the small feet. A negative polarity is located under the break in the filament. All these indicate that magnetic structure, especially the parasitic polarity near the filament, affects the shape of the filament considerably. We suppose that the large lateral feet are secondary structure to the main body of the filament because they are located in the middle of the two weak opposite polarities. The small magnetic structure under the filament may change the original configuration of magnetic field in the filament and thus causes the filament to break.

The magnetic structures near the filament are similar in the $H\beta$ magnetograms, such as the positive polarity near point A and negative polarity near point B, though the noise level here is greater. This is in agreement with the result of Zhang & Zhang (2000). Two positive polarities near the lateral feet F1 and F3 were still visible when the other parasitic polarities near the filament had almost vanished and submerged in the background noise. This may imply that

only strong magnetic polarities (stronger than 40 Gauss, for example) can expand to the higher atmosphere and that weaker magnetic polarities could not be detected in the $H\beta$ line. One reason why the noise level in the $H\beta$ magnetograms is higher than that in the photosphere is that the $H\beta$ line is formed in the chromosphere which is about 2000 km above the photosphere and there are many dynamical features in the chromosphere. Even now, the radiative transfer of the $H\beta$ line is still not understood completely. Different to the photospheric magnetograms, we can find in the $H\beta$ magnetograms magnetic signal at the location of the filament. The field strength (70 Gauss) in the filament is greater than the noise level (39 Gauss) (Fig. 4b). Considering that the filament is located far from the center of the solar disk, the line-of-sight field includes both the vertical and horizontal components of the magnetic field. Previous observations usually measured the magnetic field at various points in prominences outside the solar limb or in the background field against the solar disk in the photosphere, our observations reflect the two dimensional distribution of the line-of-sight magnetic signal inside a filament for the first time. Although another filament observed on Oct. 1, 2001 showed the same pattern of magnetic signal, we still cannot conclude that these magnetic features are common to all filaments.

The $H\beta$ 4861.34 Å line is a broad line with an equivalent width of 4.2 Å. It shows an anomalous Zeeman effect with Landé factor about 1. The core of the $H\beta$ line is formed at the height of some 1900 km (Allen 1973; Qu & Xu 2002). It is suitable for the measurement of chromospheric magnetic fields (Stenflo 1985). The passband of our filter is 0.12 Å. The line is broadened by Doppler motion in the core and by resonance damping and Stark broadening in the wing (Zhang & Zhang 2000). The quiescent filaments usually have velocities as low as (3–8) km s⁻¹ (Engvold 1986; Aulanier 1998). A filament velocity of 3 km s⁻¹ causes only a 0.05 Å displacement in the line profile. So Doppler effect is not very significant for the $H\beta$ line.

Our observations revealed the two dimensional distribution of internal magnetic field in the filament with both positive and negative polarity. The magnetic field in the filament showed evolution: sometimes a mixed polarity, sometimes a single polarity, and sometimes the polarity switches from one to the other. That the vertical magnetic field is consistent with the vertical structure is often observed in filaments. However, previous measurements showed that the magnetic field inside prominences is mainly horizontal and its direction tends to run along the long axis of the prominence. All these observations raise a question: what is the configuration of the filament? It is difficult to give a satisfactory explanation for the observational facts if we only use the dip model (Kippenhahn & Schlüter 1957) or the inverse polarity flux rope model (Kuperus & Raadu 1974). One of the possible explanations for our observational result is that the magnetic field of the filament is twisted and contains both vertical and horizontal components. That means the magnetic field in the filament may be twisted and helical. The magnetic flux ropes, which are rooted in the background field in photosphere, usually remain stable, while the field inside the filament changes all the time in both strength and direction. Another possible explanation for our observed phenomenon is that the change of the line-of-sight polarity in this filament is due to temporal change of the twisting status and projection effect of the magnetic configuration. The twisted structure of filament was also suggested by Schmieder et al. (2000) from the Doppler observation obtained using CDS on SOHO. Their Dopplergrams showed mainly red shift on the northern side of the filament and blue shift on the southern side. The twisted configuration is a promising magnetic configuration for prominences, particularly because dense material can then be naturally supported and because there is observational evidence for it (Aulanier 1998). The twisted configuration also implies the magnetic field inside

the filament is non-potential. The condensed plasma in filament may be supported by the magnetic potential energy. The filament begins to erupt when the magnetic flux rope untwists.

Our observation of the vertical magnetic field of a filament is a preliminary result and we hope that more dedicated observations of the magnetic field of filaments will be conducted by the various telescopes in the future to improve the understanding of the physical processes in the filament.

Acknowledgements We would like to thank the staff in Huairou Station for high quality observation data. The authors are also grateful to Prof. David Dewitt and Jingxiu Wang for helpful suggestions. We are indebted to Prof. Yuanyong Deng and Haimin Wang for discussion on the measurement of magnetic field. The authors thank the referee for suggestions to this paper. This work is supported by the National Science Foundation of China (NSFC).

References

- Ai G., Hu Y., 1986, *Publ. Beijing Astron. Obs.*, 8, 1
- Allen C. W., 1973, *Astrophysical Quantities*, New York: The Athlone Press
- Aulanier G., Démoulin P., 1998, *A&A*, 329, 1125
- Aulanier G., Démoulin P., Mein N., van Driel-Gesztelyi L., Mein P., Schmieder B., 1999, *A&A*, 342, 867
- Athay R. G., Quersfeld C. W., Smartt R.N., Landi Degl' innocent E., Bommier V. M., 1983, *Sol. Phys.*, 89, 3
- Babcock H. W., Babcock H. D., 1955, *ApJ*, 121, 349
- Deng Y., Ai G., Wang J. et al. 1997, *Sol. Phys.*, 173, 207
- Engvold O., Keil S., 1986, In: A. I. Poland, ed., *Coronal and Rominence Plasmas*, NASA Conference Publication, 2442, 169
- Gilbert H. R., Holzer T. E., Hundhausen A. J., 2000, *ApJ*, 537, 503
- Harvey J., 1969, Thesis, University of Colorado
- Harword R. F., 1959, *ApJ*, 130, 193
- Hirayama T., 1985, *Sol. Phys.*, 100, 415
- Kippenhahn R., Schlüter A., 1957, *Zs. Ap.*, 43, 36
- Kuperus M., Raadu M. A., 1974, *A&A*, 31, 189
- Leroy J. L., 1989, In: E. R. Priest, ed., *Dynamics and Structure of Quiescent Solar Prominences*, Dordrecht: Kluwer Academic Publishers, 77
- Martin S. F., Echols C. R., 1994, In: R. J. Retten, C. J. Schrijver, eds., *Solar Surface Magnetism*, Dordrecht: Kluwer Academic Publishers, 339
- Parker E. N., 2001, *Chin. J. Astron. Astrophys. (ChJAA)*, 1, 99
- Qu Z. Q., Xu Z., 2002, *Chin. J. Astron. Astrophys. (ChJAA)*, 2, 71
- Rust D., 1966, Thesis, University of Colorado
- Stenflo J., 1985, In: M. J. Jargyard, ed., *Measurement of Solar Vector Magnetic Field*, NASA, 263
- Schmieder B., Delannnee C., Deng Y. et al., 2000, *A&A*, 358, 728
- Tandberg-hanssen E., 1970, *Sol. Phys.*, 15, 359
- Wang T. J., Ai G. X., Deng Y. Y., 1996, *Astrophys. Reports (Publ. Beijing Astron. Obs.)*, 28, 31
- Zhang H., Ai G., Sakurai Kurukawa H., 1991, *Solar Phys.*, 136, 269
- Zhang H., Zhang M., 2000, *Sol. Phys.*, 196, 269

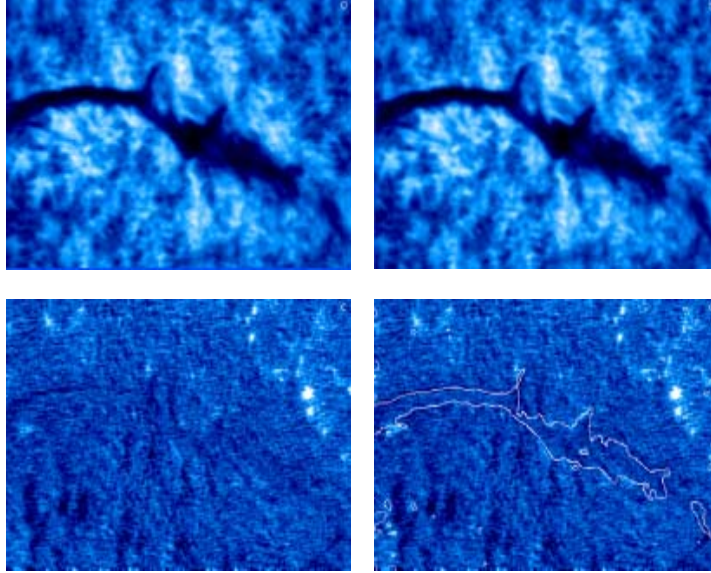


Fig. 1 Observed magnetic field of the filament at 02:02:26UT on Sep. 06, 2001. The field of view is $4.07' \times 2.77'$. (a) The left circular polarization (sum of 256 frames). The integration time is about 40 seconds. (b) The right circular polarization. It is lined up to (a) within one pixel using Fast Fourier Transform. (c) The magnetogram obtained from the difference between the right and left circular polarizations. (d) The profile of the filament (white line) is superposed on chromospheric magnetogram.

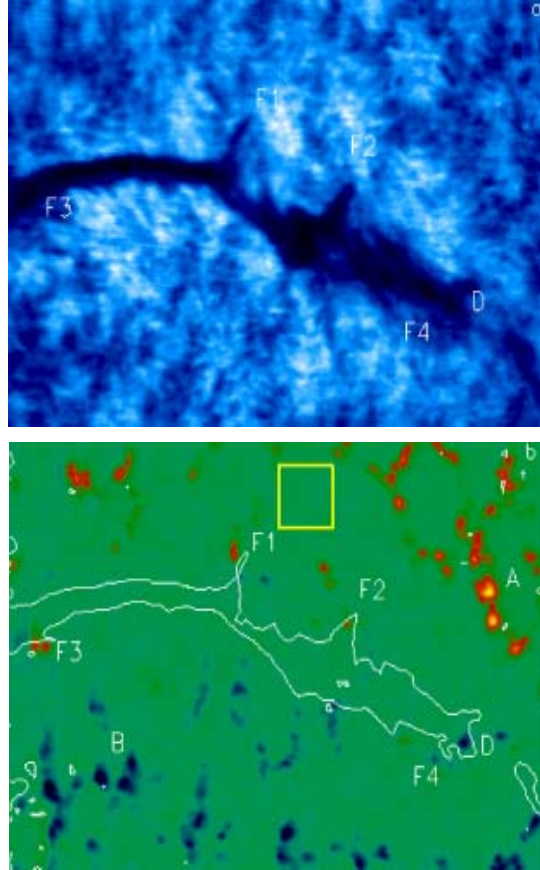


Fig. 3 (a) H β filtergram of the filament at 02:01:37 UT on Sep. 6, 2001. F1 and F2 are two large lateral feet and F3 and F4 are two smaller ones. D marks a break in the filament. North is at top and West is to the right. The field of view is $4.07' \times 2.77'$. (b) Photospheric magnetogram of the filament at 02:04:29 UT on Sep. 6, 2001. The profile of the filament is superposed on the magnetogram (white line). Red (blue) patches are positive (negative) polarities. The field of view is $4.07' \times 2.77'$. A $0.4' \times 0.4'$ region (marked by yellow square on the magnetogram of Sep. 6) with seemingly vanishing field was selected to estimate the noise. The results are: for the photospheric magnetogram (Fig. 3b) $\sigma = 3.47$ Gauss; for the H β magnetogram (Fig. 4b) $\sigma = 12.9$ Gauss.

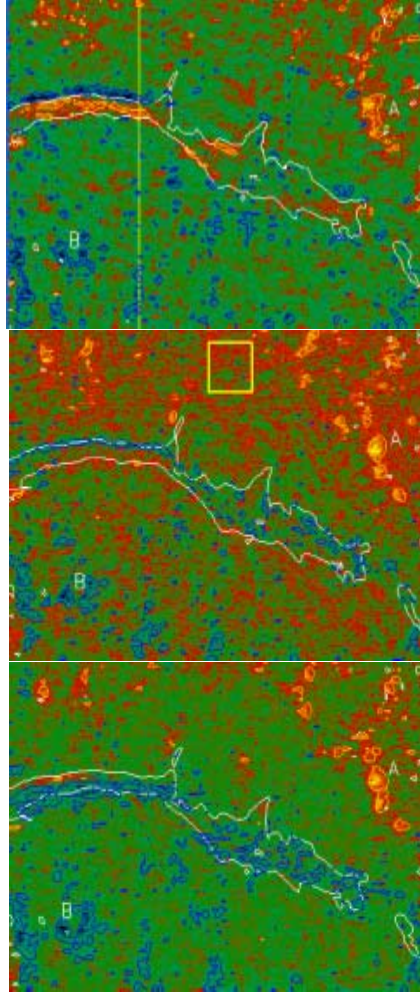


Fig. 4 H β magnetogram of the filament at 00:51:28 UT (a), 01:58:30 UT (b) and 02:58:20 UT (c) on Sep. 6, 2001. The profile of the filament are superposed on the filtergrams (bright dashed line). The yellow (blue) contours correspond to positive (negative) fields of 40 and 80 Gauss. The field of view is $4.07' \times 2.77'$.